Journal of Basic Physical Research ISSN: 2141-8403 Prints, 2141-8411 Online
Vol.14, Issue 2, October, 2025, pp. 43 – 60, Available online at https://journals.unizik.edu.ng/jbpr/

IMPACT OF MAGNETIC FIELD ON WAVES IN A ROTATING INHOMOGENEOUS MATERIAL UNDER IMPERFECT BOUNDARY AND INCLINED MECHANICAL LOAD: INHOMOGENEOUS IMPEDANCE CONSIDERATION

Augustine Igwebuike Anya *[1], Uko Ofe [2]
[1]*Department of Mathematical Sciences, Faculty of Natural and Applied Sciences, Veritas University Abuja, Bwari-Abuja, Nigeria*
[2]*Department of Pure and Applied Physics, Faculty of Natural and Applied Sciences, Veritas University Abuja, Bwari-Abuja, Nigeria*

***Corresponding Author's Emails:** anyaa@veritas.edu.ng, anyaaugustineigwebuike@gmail.com*

Abstract
We present in this investigation a Mathematical wave analysis and model for surface waves in an imperfect boundary of a rotating inhomogeneous medium under a mechanical inclination. The imperfect boundary of the material is assumed to be in the form of impedance-corrugated surface. Mathematically, we assumed this corrugation in the form of trigonometric Fourier series. While the inhomogeneous nature (both of the material and impedance parameters) is taken to be an exponentially decaying function of the material parameters. In modelling this, the dynamical equations for the rotating impedance-corrugated boundary of an inhomogeneous fibre-reinforced solid influenced by magnetic fields and inclined mechanical load were analytically derived and presented using the fundamental constitutive laws of stress-strain relations in solid Mechanics of materials. We employ the Eigenvalue method also called the normal mode analysis approach in deriving the analytical solution of the fields' distributions of the system; displacement components, and normal and shear stresses. Computational solutions in graphical forms were presented using MATHEMATICA 11 software, for the derived fields' distributions of displacement components, normal and shear stresses on the material as occasioned by the wave propagation. We observed that the impact of the inhomogeneous parameter, rotation, magnetic field, angle of inclinations, impedance-corrugated surface parameters on the fields' profiles on the material is remarkable. This is such that an increase in rotation, and angle of inclination of the medium produces an increase behavior of the fields' profiles. The magnetic field influenced the normal stress in a decreasing manner when increased whilst noting mixed behavior of the displacements and shear stress. The angles of inclinations caused upward trends to the behavior of the displacements and stresses of the wave on the medium. A resistant-like effects were observed along the normal stress components when the inhomogeneous normal impedance is increased.
***Keywords:** inhomogeneity, rotation, corrugated-impedance boundary, angle of inclination and magnetism*

Introduction

Some materials are made up of several compositions which could be phenomenally engineered by nature or artificial occurrence. Owing to this, mathematical models necessary to gain insights about the vibratory phenomena on these materials become evidently useful for scientists in the fields of engineering, geophysics, mathematics of waves, structural and material designers, amongst others. These materials are best described in two forms; isotropic and anisotropic. The considerations of only isotropic properties in a solid medium characterized in composite nature may not give accurate characteristics of the continuum responses usually involved in composites like in mechatronics devices, geophysical materials, etc.; hence the need to consider the anisotropic cases for mathematical modeling and interpretations. Composite materials like the Fibre-reinforced composites (Spencer, 1972), have flexible properties, light weight and high tensile strength which aid them to appropriate self-reinforced behaviors under some given force/area or temperature loadings. All these good qualities pave way for their great importance as applied in the engineering industries;

structural, civil, and geophysical industries. Fibre-reinforced solid could exist as a homogeneous or inhomogeneous material. Inhomogeneous fibre-reinforced material would stem from the fact that the material parameters are undergoing some decaying or growing phenomena upon deformation in the mathematical sense of it else it's a homogeneous medium.

Furthermore, wave propagation on these reinforced composites requires a mathematical model to holistically predict or deduce the behavior of such materials. These models are studied using other interacting physical parameters or quantities such as rotation (Schoenberg et al., 1973), and magnetic fields (vector field that stipulate the magnetic influences and occurrences on moving charges and magnetic materials) (Abd-Alla et al., 2017). These helps to gain favorable understanding for information processing and decision making about a wave motion and the material it propagates on or in.

Be that as it may, impedance is a measure of opposition to the flow of acoustic energy and thus, it tend to act like a resistance to the motion of mater or energy on a material. Mathematically, impedance on boundaries of materials gives conditions as linear combination of unknown functions and their rate of change defined on the boundaries, Singh, 2016). These are usually utilzed in various fields of geophysics like the electromagneto-acoustics occurrences. Aside impedance, other boundary surfaces like the corrugated surfaces could work in interactions with the impedance boundary conditions to shape the understanding of wave propagations along and across interfaces of materials. Hence, corrugated boundary surface would be understood as a series of parallel furrows and ridges whose interaction in mechanical propagation of waves yields to several effects across interfaces (Asano, 1966). Mathematically, we assumed this as a Fourier trigonometric series prescribed at the boundary of surfaces.

Undoubtedly, other authors in the literatures have contributed to further the study on this corrugated boundary and other related wave propagation occurrences: (Singh, 2022; Singh and Tomar, 2008; Singh et al., 2015; Singh, et al., 2018; Das, et al., 1992; Abd-Alla et al., 2016; Chattopadhyay et al., 1975; Roy et al., 2017; Singh and Sindhu, 2011; Gupta, 2014; Anya et al. 2018; Anya and Khan, 2019; Anya and Khan, 2020, Anya and Khan, 2022; Maleki and Jafarzadeh, 2023; Chowdhury et al., 2021; Singh and Kaur, 2020; Sahu et al., 2022; Giovannini, 2022; Anya and Khan, 2019; Giovannini, 2022 and Rakshit et al., 2021 and 2022; Barak and Dhankhar, 2023 and Barak et al., 2024) as an individual or part examination of the interacting physical quantities especially of inhomogeneity, mechanical inclinations, rotation of the medium, micropolar effects etc., rather than as in combined impacts obtainable in this present investigation where inhomogeneous impedance and mechanical inclination at the boundary holds.

In spite of the above given literatures and materials, the present investigation is geared towards developing a mathematical framework and analysis to aid the understanding associated with propagation of surface waves in a rotating corrugated-impedance boundary of an inhomogeneous magneto-elastic fibre-reinforced solid under mechanical inclinations. The equations of motion are derived by inculcating these physical quantities of rotation, magnetic field, inhomogeneity of the material and as well as employing dimensionless parameters as a convenience. The eigenvalue method also called the normal mode analysis was utilized to find the analytical solutions to the equations of motion. Corrugated-impedance surface conditions were employed at the boundary whilst taking the impedance parameter to be inhomogeneous with an underlying angle of inclination of the material to finding a complete solution to the displacement components and stresses of the wave on the material. These analytical results

were graphically depicted and presented for a chosen fibre-reinforced solid. We observed that these interacting physical parameters have enormous impacts to the displacements of the waves and stresses on the solid half-space.

Materials and Methods

Mathematical Model and Formulations

The constitutive stress-strain equations for a homogeneous fibre–reinforced elastic anisotropic half-space (Spencer, 1972) and magnetic force (Abd-Alla et al., 2017; and Anya et al., 2023) are presented below:

$$\tau_{ij} = \lambda\varepsilon_{kk}\delta_{ij} + 2\mu_T\varepsilon_{ij} + \alpha(d_k d_m \varepsilon_{km}\delta_{ij} + \varepsilon_{kk} d_i d_j) + 2(\mu_L - \mu_T)(d_i d_k \varepsilon_{kj} + d_j d_k \varepsilon_{ki}) + \beta(d_k d_m \varepsilon_{km} d_i d_j), \quad (1)$$

$$F_i = \mu_0 H_0^2 \left(e_{,1} - \varepsilon_0 \mu_0 \ddot{u}_1, e_{,2} - \varepsilon_0 \mu_0 \ddot{u}_2, 0\right) = (F_1, F_2, F_3), i = 1,2,3, \quad \varepsilon_{ij} = \tfrac{1}{2}\left(u_{i,j} + u_{j,i}\right) \quad (2)$$

In these equations above, τ_{ij}, ε_{ij}, u_i, δ_{ij}, λ, (α, β, $(\mu_L - \mu_T)$) and F_i are the stress tensor, strain tensor, displacement vector, Kronecker–delta function, Lames constant, fiber-reinforced parameters and magnetic force respectively. We take $d = (d_1, d_2, d_3)$ such that $d = (1,0,0)$ entails the fibre directions. $H_i = H_0\delta_{i3} + h_i$, $\mathrm{h_i} = (0\ ,\ 0, -\mathrm{e})$, $\mathrm{e} = \mathrm{u_{i,i}}, \mathrm{i} = \mathrm{i}, 2$ h_i is induced magnetic field, ε_o is electric permeability. The material is presume to lie in the x_1x_2 – plane. $h_i(x_1, x_2, x_3) = -u_{k,k}\delta_{i3}$. H_i is magnetic vector field and μ_o is the magnetic permeability owing to Maxwell's electromagnetism. Considering the presence of magnetic fields and rotation of the medium, (Schoenberg et al.1973), the dynamical equation in homogeneous form becomes:

$$\tau_{ij,j} + F_i = \rho\{\ddot{u}_i + \Omega_j u_j \Omega_i - \Omega^2 u_i - 2\varepsilon_{ijk}\Omega_j \dot{u}_k\} \quad (3)$$

ε_{jim} denote the Levi–Civita tensor and the given index after comma connotes partial derivatives with respect to coordinate space and the superscript dot stipulates partial derivative with respect to time. Hence, since we are considering the deformation in the x_1x_2–plane, it implies $x_3 = 0$ such that $u_1 \neq u_2 \neq u_3 \neq 0$. We also assume the rotation $\Omega = \Omega(0,0,1)$ i.e. the rotation of the media is about the x_3-axis.

Furthermore, consider the case that the inhomogeneity of the material grows or decay slowly and that its rate of growth or decay is proportional to its value at that point. In the present problem we have considered exponentially decaying inhomogeneous fibre-rinforced solid. This entails that the elastic module, elastic parameters, and density assumes the following forms (Khan et al., 2015) and Munish et al., 2016):

$(\alpha, \beta, \lambda, \mu_T, \mu_L, \rho) = (\alpha_0, \beta_0, \lambda_0, \mu_{T_0}, \mu_{L0}, \rho_0)e^{-mx_2}$, m represent the inhomogeneous quantity.

In addition, considering the fact the tensors are symmetric, and that inhomogeneity of the medium are incorporated in the formulations, Eq. (3) in component forms becomes the equations of motion below:

$$(\lambda + 2\alpha + 4\mu_L - 2\mu_T + \beta + \mu_0 H_0^2)u_{1,11} + (\alpha + \lambda + \mu_L + \mu_0 H_0^2)u_{2,21} + \mu_L u_{1,22} - m\mu_T\left(u_{1,2} + u_{2,1}\right) = \{\rho + \varepsilon_0\mu_0^2 H_0^2\}\ddot{u}_1 - \rho\Omega^2 u_1 - 2\Omega\dot{u}_2\}, \quad (4)$$

$$(\alpha + \lambda + \mu_L + \mu_0 H_0^2)u_{1,12} + \mu_L u_{2,11} + (\lambda + 2\mu_T + \mu_0 H_0^2)u_{2,22} - m(\lambda + \alpha)u_{1,1} - m(\lambda + 2\mu_T)u_{2,2} = \{\rho + \varepsilon_0\mu_0^2 H_0^2\}\ddot{u}_2 - \rho\{\Omega^2 u_2 + 2\Omega\dot{u}_1\}, \quad (5)$$

$$\mu_L u_{3,11} + \mu_T u_{3,22} - m\mu_T u_{3,2} = \rho\ddot{u}_3. \quad (6)$$

We can rewrite Eqs. (4-6) in the form:

$$A_1 u_{1,11} + A_2 u_{2,21} + A_3 u_{1,22} - mA_4\left(u_{1,2} + u_{2,1}\right) = \{\{\rho + \varepsilon_0\mu_0^2 H_0^2\}\ddot{u}_1 - \rho(\Omega^2 u_1 + 2\Omega\dot{u}_2)\}, \quad (7)$$

$$A_2u_{1,12}+A_3u_{2,11}+A_5u_{2,22}-mA_6u_{1,1}-mA_7u_{2,2}=\{\{\rho+\varepsilon_0\mu_0^2H_0^2\}\ddot{u}_2-\rho(\Omega^2u_2-2\Omega\dot{u}_1)\}, \quad (8)$$

$$A_3u_{3,11}+A_4u_{3,22}-mA_4u_{3,2}=\rho\ddot{u}_3. \quad (9)$$

Here,

$A_1=(\lambda+2\alpha+4\mu_L-2\mu_T+\beta+\mu_0H_0^2), A_2=(\alpha+\lambda+\mu_L+\mu_0H_0^2), A_3=\mu_L, A_4=\mu_T, A_5=(\lambda+2\mu_T+\mu_0H_0^2),$ $A_6=(\lambda+\alpha), A_7=(\lambda+2\mu_T)$. We consider the following dimensionless quantities below as a convenience:

$(x_1',x_2',u_1',u_2')=c_0(x_1,x_2,u_1,u_2),\ (t')=c_0^2\,\mathrm{t},\ \Omega'=\Omega/c_0^2,\ \sigma_{ij}'=\sigma_{ij}/\rho c_0^2, c_0^2,=A_1/\rho$. When we employ the dimensionless quantities into Eqs (7-9) and by removing the prime, we obtain the following:

$$u_{1,11}+A_{12}u_{2,21}+A_{13}u_{1,22}-mA_{24}\left(u_{1,2}+u_{2,1}\right)=\{\{1+\varepsilon_0\mu_0^2H_0^2/\rho\}\ddot{u}_1-\rho\Omega^2u_1-2\rho\Omega\dot{u}_2\}, \quad (10)$$

$$A_{12}u_{1,12}+A_{13}u_{2,11}+A_{15}u_{2,22}-mA_{26}u_{1,1}-mA_{27}u_{2,2}=\{\{1+\varepsilon_0\mu_0^2H_0^2/\rho\}\ddot{u}_2-\rho\Omega^2u_2+2\rho\Omega\dot{u}_1\}, \quad (11)$$

$$A_{13}u_{3,11}+A_{14}u_{3,22}-mA_{24}u_{3,2}=\ddot{u}_3 \quad (12)$$

Where; $(A_{12},A_{13},A_{14},A_{15},A_{16},A_{17})=((A_2,A_3,A_4,A_5,A_6,A_7)/A_1$ and $(A_{24},A_{26},A_{27})=(A_{14},A_{16},A_{17})\rho^{1/2}/A_1^{3/2}$.

Methods

Analytical Solution of the Problem

This section provides us with the need to consider a clear cut normal mode method or the eigenvalue approach for the rotating impedance-corrugated surface boundary of the inhomogeneous magneto-elastic fibre-reinforced half-space $x_2<0$ under mechanical inclined angle. Following this, we assume the normal mode approach is adopted such that the waves have the displacements:

$$u_j=(\hat{u}_j(x_2))e^{\omega t+ibx_1},\ j=1,2,3. \quad (11)$$

Employing Eq (11) into Eqs (10-12), we achieve a system of three differential equations in the x_2-direction as:

$$(A_{13}D^2-mA_{24}D-b^2-K)\hat{u}_1+(iA_{12}bD-mA_{24}bi-2\rho\Omega\omega)\hat{u}_2=0, \quad (12)$$

$$(iA_{12}bD-mbiA_{26}+2\rho\Omega\omega)\hat{u}_1+(A_{15}D^2-mA_{27}D-A_{13}b^2-K)\hat{u}_2=0, \quad (13)$$

$$(\mathrm{A}_{14}D^2-mA_{24}D-(\mathrm{A}_{13}b^2+\rho\omega^2)\hat{u}_3=0. \quad (14)$$

Here, $K=(1+\varepsilon_0\mu_0^2H_0^2/\rho)\omega^2+\rho\Omega^2)$. For non- trivial solution, Eqs. (12-13) become the quartic equation below; which is a fourth order ordinary differential equation. In the case of homogenous material, this will produce a quadratic homogenous characteristic equation in D^2 or simply second order differential equation in D^2.

$$(C_{11}D^4+C_{12}D^3+C_{13}D^2+C_{14}D+C_{15})(\hat{u}_1,\hat{u}_2)=0. \quad (15)$$

Here $C_{1i}, i=1,2,3,4,5$ denote complex coefficients which are dependent on the material parameters. If $\ell_i, i=1,2,3,4$ be positive real roots of the characteristics of Eq (15), the normal mode analysis stipulates that we can get the solution:

$$(\hat{u}_1,\hat{u}_2)=(M_n,M_{1n})e^{-\ell_n x_2}n=1,2,3,4., \quad (16)$$

Here, M_n and M_{1n} are parameters which are dependent on the wavenumber b in the x_1 coordinate and direction. Aslo, ω denote the complex frequency of the waves. Introducing Eq (16) into the Eqs (10-11), the following equation are derived:

$$M_{1n}=P_{1n}M_n, \quad (17)$$

$$P_{1n}=(A_{13}\ell_n^2+mA_{24}\ell_n-b^2-K-(2\rho\Omega\omega-iA_{12}b\ell_n-mbiA_{26})/(A_{15}\ell_n^2-A_{13}b^2+mA_{27}\ell_n-K+(2\rho\Omega\omega+iA_{12}b\ell_n+mbiA_{24})$$

where; $n=1,2,3,4$. Eq.(14) which is uncoupled take the solution: $u_3=(Ee^{-\hbar_1x_2}+E_1e^{\hbar_2x_2})e^{\omega t+ibx_1}$.

Here, $\hbar_{1,2} = 1/2(mA_{24}/A_{14} \pm ((mA_{24}/A_{14})^2 + 4(A_{13}b^2 + \rho\omega^2)/A_{14})^{1/2})$ denote the roots of the uncoupled Eq. (14). Mathematically and physically speaking, the existence of transverse components and boundedness of solution leads the uncoupled Eq. (14) to take the form: $u_3 = Ee^{-\hbar_1 x_2 + \omega t + ibx_1}$. Thus, the solutions for the total displacement functions and stresses on the impedance-corrugated inhomogeneous fibre-reinforced material in the dimensionless forms yields:

$u_1 = M_n e^{-\ell_n x_2 + \omega t + ibx_1}$, $u_2 = P_{1n} M_n e^{-\ell_n x_2 + \omega t + ibx_1}$, $u_3 = Ee^{-\hbar_1 x_2 + \omega t + ibx_1}$,

$\tau_{11} = \{ib(1-(\mu_0 H_0^2/A_1)) - \ell_n P_{1n} A_{16}\} M_n e^{-(\ell_n + m)x_2 + \omega t + ibx_1}$, $\tau_{22} = \{ibA_{16} - \ell_n P_{1n} A_{17}\} M_n e^{-(\ell_n + m)x_2 + \omega t + ibx_1}$,

$\tau_{12} = (ibP_{1n} - \ell_n) A_{13} M_n e^{-(\ell_n + m)x_2 + \omega t + ibx_1}$, $\tau_{21} = A_{13}(ibP_{1n} - \ell_n) M_n e^{-(\ell_n + m)x_2 + \omega t + ibx_1}$, $\tau_{23} = \{-\ell_n A_{14} E\} M_n e^{-(\hbar_n + m)x_2 + \omega t + ibx_1}$.

The above displacement and stress distributions are presented in tensor notation such that $n = 1, 2, 3, 4.$

Impedance-Corrugated Surface Conditions and Applications of Mechanical Inclination

Suppose we represent the equation of the corrugated surface of the inhomogenous fibre-reinforced medium in the form $x_2 = \xi(x_1)$ where $\xi(x_1) = \sum_{l=1}^{\infty} (\xi_l e^{ilbx_1} + \xi_{-l} e^{-ilbx_1})$ follows (Asano, 1966). So $\xi(x_1)$ connotes a trigonometric Fourier series which is periodic and do not depend on the coordinate x_3. Also, η_l and η_{-l} fully denote the Fourier expansion coefficients and l is the series expansion order. The parameters a, F_l and I_l are defined to take the form $\xi_1^{\pm} = a/2$, $\xi_l^{\pm} = (F_l + I_l)/2,\ l = 2, 3...$, and $\xi(x_1) = a\cos bx_1 + F_2 \cos 2bx_1 + I_2 \sin 2bx_1 + ... + F_l \cos lbx_1 + I_l \sin lbx_1$, , F_l and I_l represent the Fourier cosine and sine Fourier coefficients respectively. Hence, we take the nature of the corrugated boundary surface in the form of cosine terms, that is, $\xi(x_1) = a\cos bx_1$. Here, a denote the amplitude of the corrugated boundary while b is the wavenumber linked to the corrugated boundary surface such that the corrugated boundary surface assume the wavelength $2\pi/b$.

i. The displacements at the surface can be taken in the form:
   $u_1 = 0,$ and $u_2 = 0,$ at $x_2 = \xi(x_1)$, for all x_1 and t

ii. Also, the stresses w.r.t $x_2 = \xi(x_1)$ for the coupled equations are assumed in the form:
   $\tau_{22} - \xi'(x_1)\tau_{21} + \bar{\tau}_{ij} + \omega Z_2^* u_2 = -F_1 e^{\omega t + ibx_1} \cos\theta,$
   This shows that the normal stress condition would finally take the form:
   $\tau_{22} + \bar{\tau}_{22} - \xi'(x_1)\tau_{21} + \omega Z_2^* u_2 = -F_1 e^{\omega t + ibx_1} \cos\theta,$
   $\Rightarrow \tau_{22} + \mu_0 H_0^2 (u_{1,1} + u_{2,2}) - \xi'(x_1)\tau_{21} + \omega Z_2^* u_2 = -F_1 e^{\omega t + ibx_1} \cos\theta,$
   where $\bar{\tau}_{22} = \mu_0 H_0^2 (u_{1,1} + u_{2,2})$ (Abd-Alla et al., 2013; Anya et al.. 2023 and Azhar et al., 2023) represents the additional term on the surface of the fibre- reinforced medium due to Maxwell's stresses while the tangential stress condition or shear stress component condition is: $\tau_{12} - \xi'(x_1)\tau_{11} + \omega Z_1^* u_1 = -F_1 e^{\omega t + ibx_1} \sin\theta$, for all x_1 and t.

iii. And thus, the uncoupled equation takes the condition:
   $u_3 = 0,$ and $\tau_{23} = 0$, at $x_2 = \xi'(x_1)$, for all x_1 and t.

Moreover, τ_{12} and normal stress τ_{22} are mathematically proportional to the tangential and vertical displacement components times frequency, respectively. Considering this, we take as an application to relate the impedance-corrugated boundary conditions of the material and the inclined mechanical angle (Ailawalia et al., 2015) This produce (ii) above. Z_1^* and Z_2^* are the proportional coefficients called impedance parameters. We suppose that these impedance parameters are equally inhomogeneous such that $Z_1^* = Z_1 e^{-mx_2}, Z_2^* = Z_2 e^{-mx_2}$. The traction free impedance-corrugated boundary conditions are retrieved if $F_0 = 0.$ Thus, the application of

$F_1 = F_0 e^{-mx_2}$, in the boundary conditions for the coupled equations, the stress and displacements components, yields the following;

$$M_n = 0, \tag{18}$$

$$P_{1n} M_n = 0, \tag{19}$$

$$\{ibA_{16} - \ell_n P_{1n} A_{17}\} e^{-\ell_n \xi(x_1)} M_n + ab \sin bx_1 \{(ibP_{1n} - \ell_n) A_{13}\} e^{-\ell_n \xi(x_1)} M_n + \{\omega P_{1n} Z_2 M_n + \mu_0 H_0^2 (ib - \ell_n P_{1n})\} e^{-\ell_n \xi(x_1)} M_n = -F_0 \cos\theta, \tag{20}$$

$$\{\{ibP_{1n} - \ell_n\} A_{13} M_n + ab \sin bx_1 \{ib(1 - (\mu_0 H_0^2 / A_1)) - \ell_n P_{1n} A_{16}\} M_n + \{\omega Z_1\}\} M_n e^{-\ell_n \xi(x_1)} = -F_0 \sin\theta, \qquad n = 1,2,3,4. \tag{21}$$

By solving for $M_n, n = 1,2,3,4$ in Eqs. (18-21), the complete developed analytical solutions of the displacement components of the waves and stresses (normal and shear stresses) on the inhomogeneous magneto-elastic fibre-reinforced impedance-corrugated under mechanical inclined angles are achieved. Rayleigh wave novel dispersion equation can be deduced for the model problem if we consider a nontrivial solution of the homogeneous system of equations such that $|M_n| = 0, n = 1,2,3,4$ in equations (18-19).

Results and Discussion

In this section, efforts were made by using the material constants of fibre-reinforment Sunita et al., 2015) and other physical parameters given below to examine the effects of magnetic fields, rotation, impedance-corrugated surface, inhomogeneity (both of material and impedance), applied force and inclination angles on the derived fields' distributions of the system; normal and shear stresses, and the displacement components of the wave propagation on the material. In doing so, the various profiles of these fields' distributions and their analysis are thus, presented graphically in figures (1-9) below:

$\mu_T = 2.46 \times 10^{10}\, kg\, m^{-1} s^{-2}; \mu_L = 5.66 \times 10^{10}\, kg\, m^{-1} s^{-2}; \lambda = 5.65 \times 10^{10}\, kg\, m^{-1} s^{-2}; \rho = 2660 kg\, m^{-3};$
$\alpha = -1.28 \times 10^{10}\, kg\, m^{-1} s^{-2}; \beta = 220.9 \times 10^{10}\, kg\, m^{-1} s^{-2}; \omega = (0.02 + \mathrm{i})\,\mathrm{rad/s}; H_0 = 1000 A/m; t = 0.5\mathrm{s}; \theta = 30^0$
$b = 0.6; m = 0.50; \Omega = 0.020 rad/s; a = 0.290; \mathrm{F}_0 = 0.000005 N; x_1 = 1.2m; \mathrm{Z}_1 = 0.005; \mathrm{Z}_2 = 0.007.$

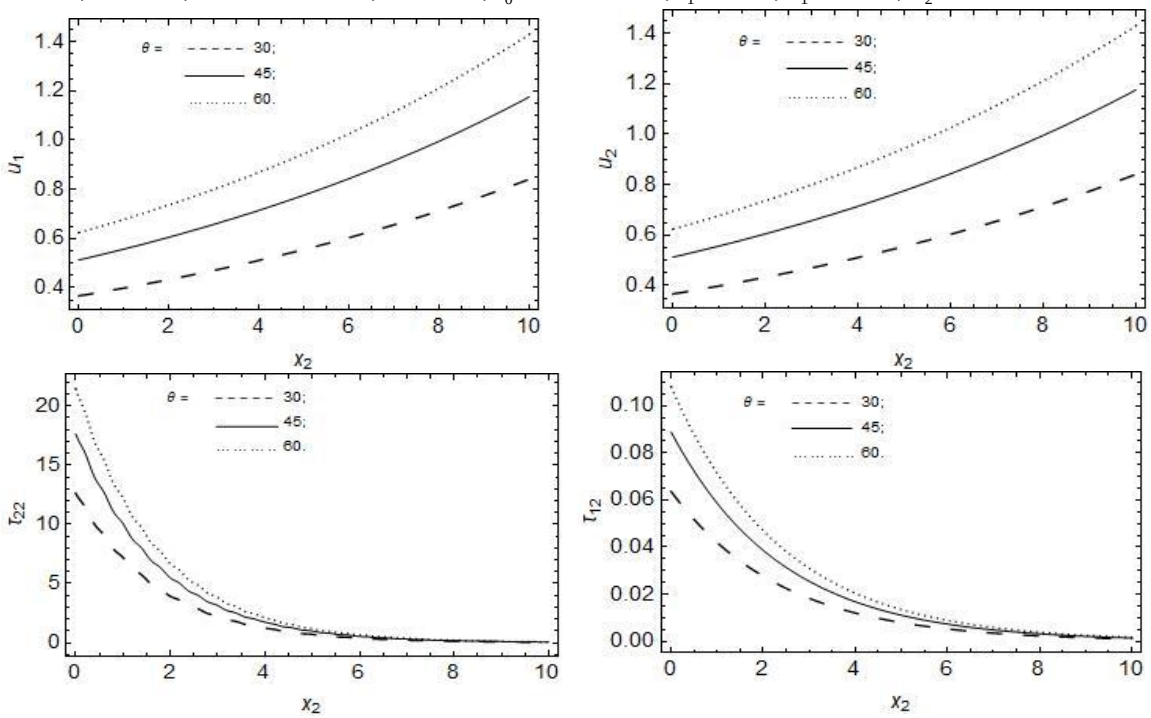


Fig. 1: Impact of distinct angles of mechanical inclinations θ in degrees on the displacement components $u_i, i = 1,2$, normal stress τ_{22} and shear stress τ_{12} versus x_2 in meters.

Fig. 1 demonstrates the variations of the inclined mechanical angle θ in degrees on the displacement components $u_i, i = 1,2$, normal stress τ_{22} and shear stress τ_{12} as against the x_2 coordinate with constant physical parameters of applied mechanical inclination (applied force) F_0, magnetic fields H_0, inhomogeneous parameter m, rotation of the medium Ω, inhomogeneous impedance Z_i, and corrugated surface parameters a, b at a given time t on the fibre-reinforced inhomogeneous material. We observe that there is a consistency in change in the stresses and displacements of the wave on the material as the angles of inclination increases. However, the stresses tends to have a mode of propagation or profile different from the displacement profiles. This is such that for an increase in the angle of inclination θ and $x_2 \leq 6$, a more visible increase in behavior is witnessed for the stresses unlike for $x_2 \geq 6$, while the displacement components displayed a clear increase as the angles increases. The maxima values of the stresses are witnessed near the origin and for $\theta = 60^0$, while the maxima values for the displacements occur near $x_2 = 10$. This wholesomely show that the angle of inclination of the model increase propagation and modulation of the wave stresses and displacements on the fibre-reinforced inhomogeneous material when increased.

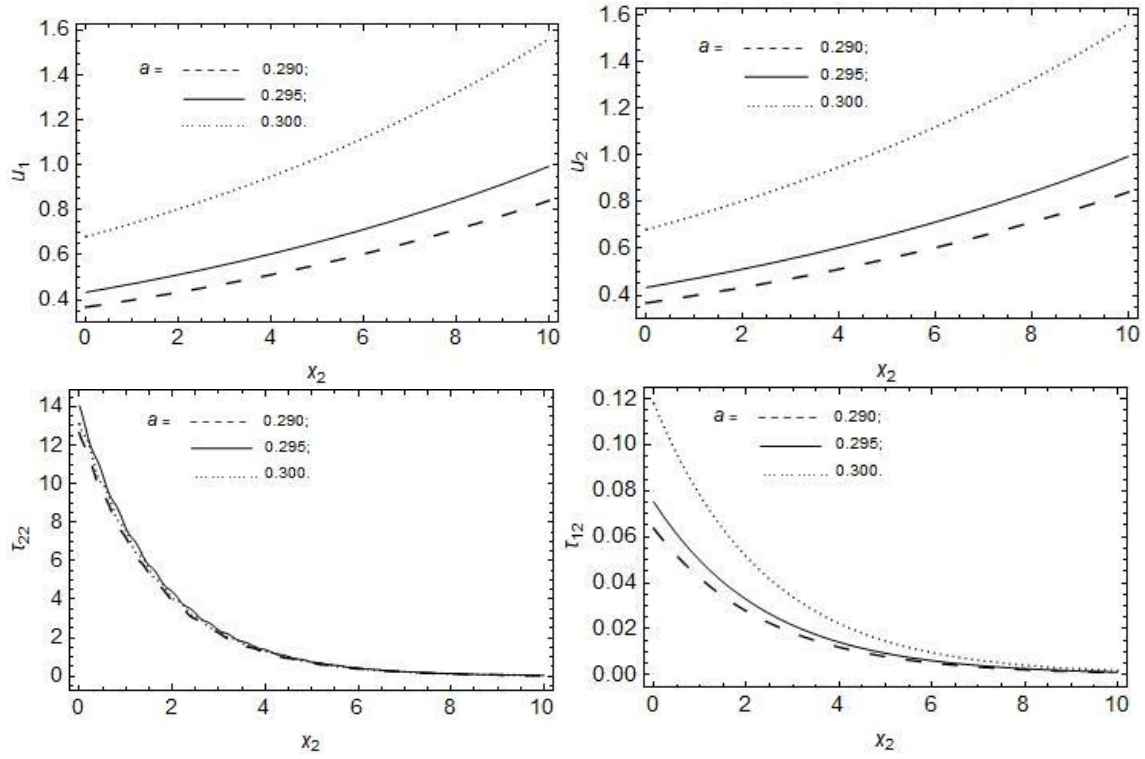


Fig. 2: *Impact of distinct amplitudes a of corrugation on the displacement components* $u_i, i = 1,2$, *normal stress* τ_{22} *and shear stress* τ_{12} *versus* x_2 *in meters.*

Consequently, Fig. 2 stipulates the impact of the distinct amplitudes a of corrugation on the displacements $u_i, i = 1,2$, normal stress τ_{22} and shear stress τ_{12} versus x_2 coordinate in meters whereby other interacting physical quantities or physical parameters of inclined angle θ, applied mechanical inclination parameter (applied force) F_0, magnetic fields H_0, inhomogeneous parameter m, rotation of the medium Ω, inhomogeneous impedance Z_i, and

corrugated surface parameter b are held in fixed manner at a given time t on the material. Observations are made such that the amplitude a, of the corrugated surface increase the shear stress τ_{12} and displacement of the wave propagation on the medium especially when increased while the normal stress τ_{22} demonstrate mixed (increase and decrease) behavior at this instance. Thus we posit that similar analysis obtainable from Fig. 1 for the maxima values could be associated to Fig. 2 except for the normal stress τ_{22} whose maximum is near the origin and for $a = 0.295$. Also, τ_{12} maximum value is obtained near the origin but for $a = 0.300$.

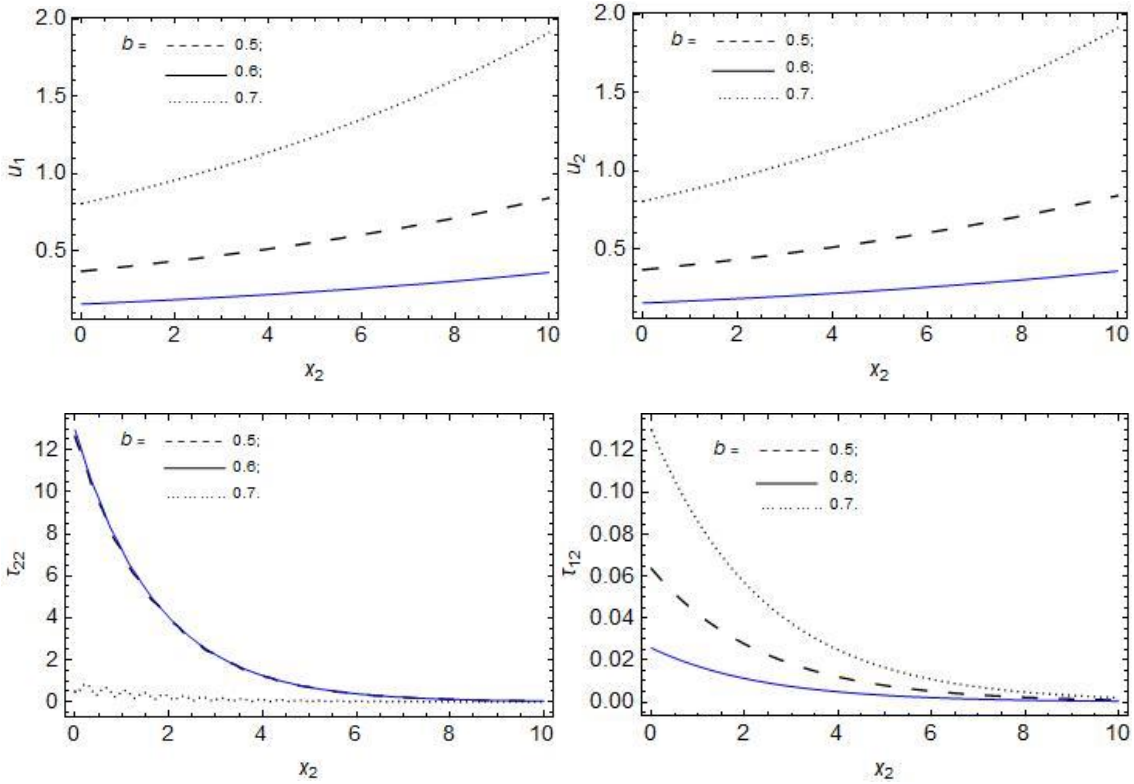


Fig. 3: *Impact of distinct wave number* b *on the displacement components* $u_i, i = 1,2$, *normal stress* τ_{22} *and shear stress* τ_{12} *versus* x_2 *in meters.*

Subsequently, Fig. 3 shows the effects of the distinct wave number b on the displacements $u_i, i = 1,2$, normal stress τ_{22} and shear stress τ_{12} versus x_2 coordinate in meters. This is such that other interacting physical quantities or physical parameters of inclined angle θ, applied mechanical inclination parameter (applied force) F_0, magnetic fields H_0, inhomogeneous parameter m, rotation Ω of the medium, inhomogeneous impedance $Z_i, \mathrm{i} = 1,2$ and amplitude a of the wave are in steady application on the fibre-reinforced inhomogeneous material at a given time t. The wave number associated with the corrugated surface caused a sharp upward increase in the shear stress τ_{12} and mixed behaviors on the normal stress and displacement profiles $u_i, i = 1,2$, of the wave when increased at this instance. However, it is never the same for the normal stress τ_{22} profile, that is, τ_{22} demonstrate a decrease behavior in an oscillating manner when $b = 0.7$ and for $x_2 \le 0.4$. The maxima for stresses are obtained near the origin, for different values of the wave number b. For instance, the maximum for the normal stress at $b = 0.6$ while the shear stress occur at $b = 0.7$. The maxima for the displacement profiles are similar to the analysis on maxima obtainable at Fig. 1. Thus, we can deduce that an increase

in the wave number increase the displacement distributions and the shear stress while causing mix behavior to the normal stress profile.

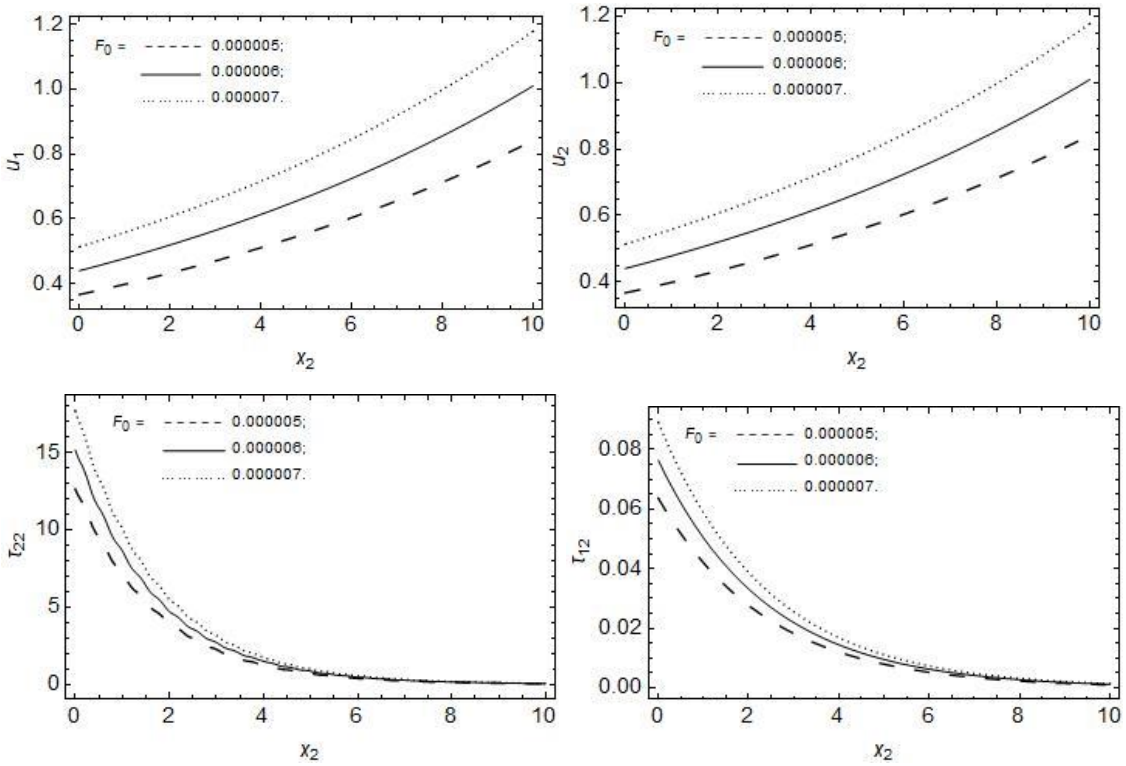


Fig. 4: Impact of distinct mechanical inclined parameter F_0 (applied force) on the displacement components $u_i, i = 1,2$, normal stress τ_{22} and shear stress τ_{12} versus x_2 in meters.

Nevertheless, Fig. 4 entails the impact of distinct mechanical inclined parameter F_0 (applied force) on the displacements $u_i, i = 1,2$, normal stress τ_{22} and shear stress τ_{12} versus x_2 coordinate in meters, especially at a constant application of other interacting physical quantities or physical parameters of inclined angle θ, magnetic fields H_0, inhomogeneous parameter m, rotation Ω of the medium, inhomogeneous impedance $Z_i, \mathrm{i} = 1,2$ and corrugated surface parameters a, b of the wave on the inhomogeneous material at a given time t. In Fig. 4, we can observe that an increase in the mechanical inclined parameter or applied force F_0 leads to an increase in all the fields' profiles on the material, that is, the Stresses and displacement profiles increases. This would mean that the force acted as a push to the material body and thus leading to increase in energy of the system thereby causing more propagation of the wave phenomenon. Similar analysis for the maxima values in Fig. 1 can be performed in Fig. 4. with F_0 in focus.

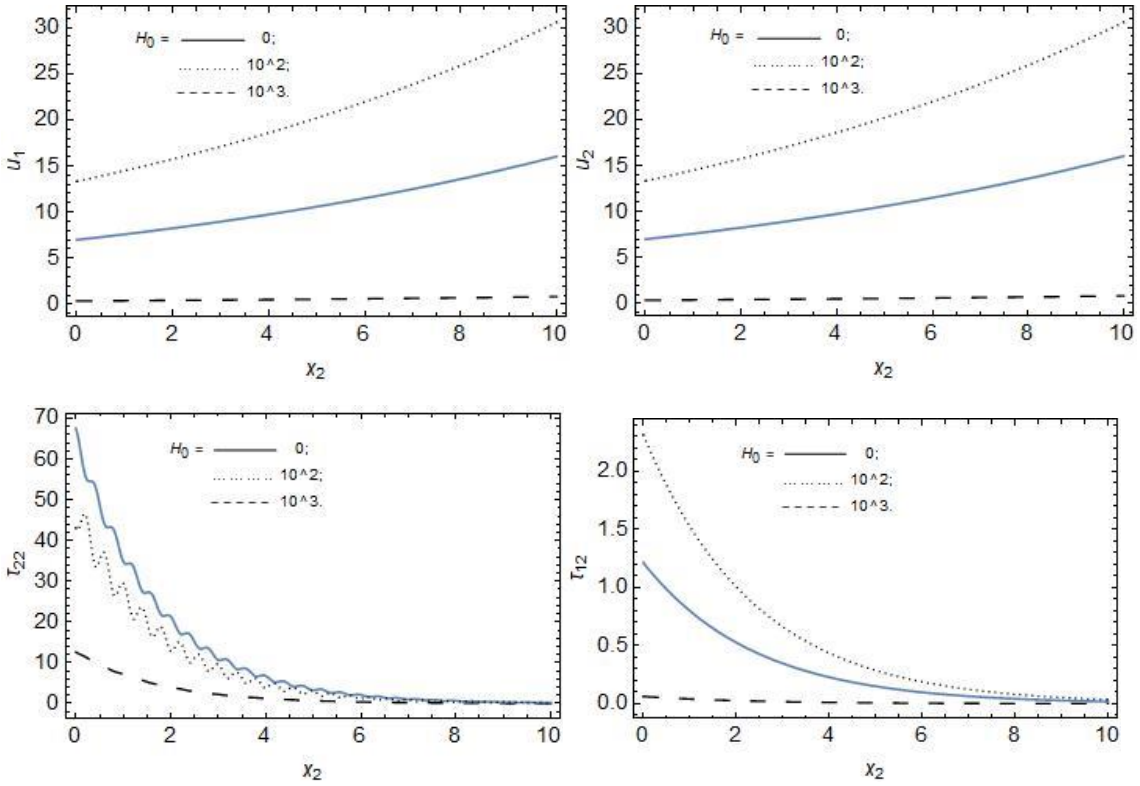


Fig. 5: Impact of distinct magnetic field $H_0(A/m)$ on the displacement components $u_i, i=1,2$, normal stress τ_{22} and shear stress τ_{12} versus x_2 in meters

Furthermore, Fig. 5 depicts the impact of distinct magnetic field $H_0(A/m)$ on the displacements $u_i, i=1,2$, normal stress τ_{22} and shear stress τ_{12} versus x_2 coordinate in meters with the considerations that the interacting physical quantities or physical parameters of inclined angle θ, mechanical inclined parameter F_0 (applied force), inhomogeneous parameter m, rotation Ω of the medium, inhomogeneous impedance $Z_i, \mathrm{i}=1,2$ and corrugated surface parameters a, b are applied in steady form at a given time t on the material. Observations made connotes that the magnetic field H_0 developed mixed behavior (increase and decrease) on the displacements $u_i, i=1,2$ and the shear stress τ_{12} when varied in an increase manner on the material. While the normal stress τ_{22} witnessed a consistent decrease for increase in H_0 on the material. Also, some oscillations occur when the applied H_0 values become small. The maximum value for the normal stress τ_{22} is near the origin when there is no or negligible magnetic field as compared with the rest of the other profiles ($u_i, i=1,2$ and τ_{12}) that attains maxima values at $H_0=100$. Physically speaking, we can infer that the wave distribution normal to the fibre-reinforced body will witness a decrease in propagation on the material when the magnetic force is high while the tangential wave distributions and the displacements of the waves shall witness some form of mixed behavior in modulations if the magnetic field increase.

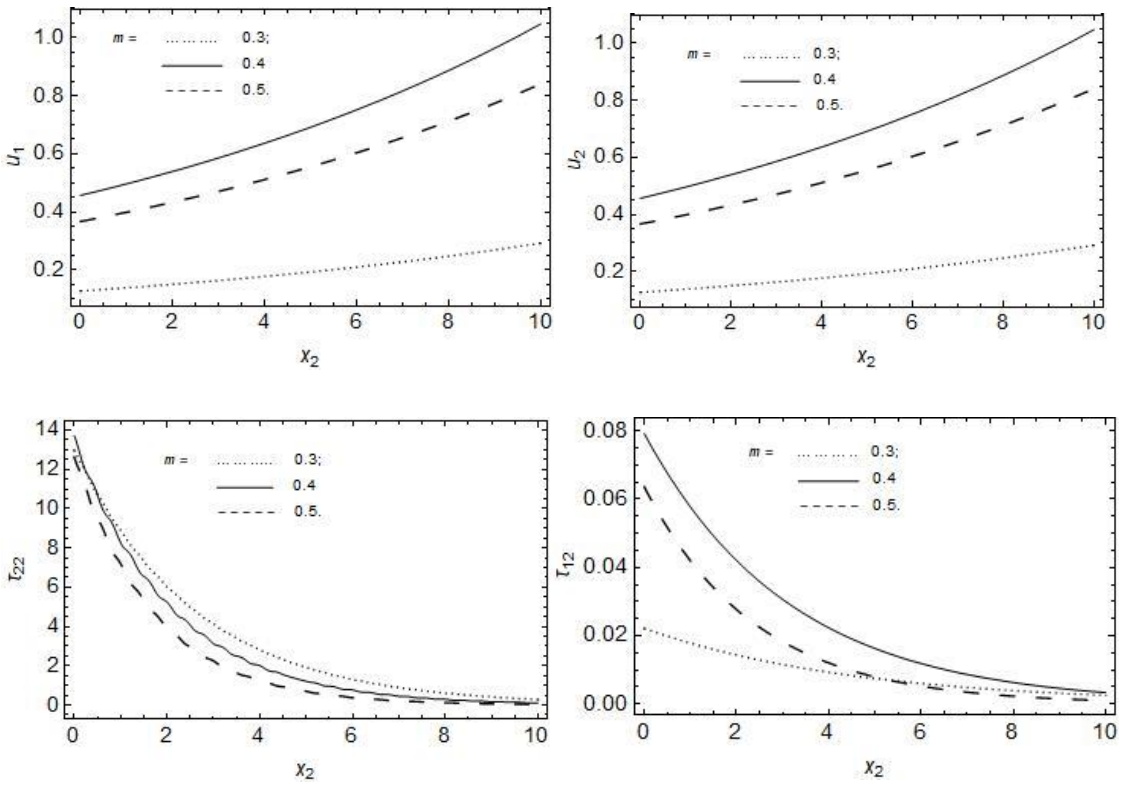


Fig. 6: Impact of distinct inhomogeneous parameter m on the displacement components $u_i, i = 1,2$, normal stress τ_{22} and shear stress τ_{12} versus x_2 in meters.

Moreover, Fig. 6 demonstrate the effects of distinct inhomogeneous parameter m on the displacements $u_i, i = 1,2$, normal stress τ_{22} and shear stress τ_{12} versus x_2 coordinate in meters when the interacting physical quantities or physical parameters of inclined angle θ, mechanical inclined parameter F_0 (applied force), magnetic field $H_0(A/m)$, rotation Ω of the medium, inhomogeneous impedance $Z_i, \mathrm{i} = 1,2$ and corrugated surface parameters a, b are held constant at a given time t on the material. We observed that increase in the inhomogeneity m on the material decrease the normal stress τ_{22} on the material while noting mixed behavior in the domain $0 < x_2 \leq 1$where the maximum value lies. However, inhomogeneity m of the material caused clear mixed behavior (increase and decrease) on the displacements $u_i, i = 1,2$ and the shear stress τ_{12} when increased. Similar analysis for the maxima of $u_i, i = 1,2$ and τ_{12} follows from Fig. 1 with inhomogeneity m of the material in focus. Physically speaking, this stipulate that as the material deforms, there is a supposedly gradual malleability or change in characteristics or state of the material and hence infusing a room for mixed or consistency in behavior of the displacements and stresses of the waves propagating on the fibre-reinforced body.

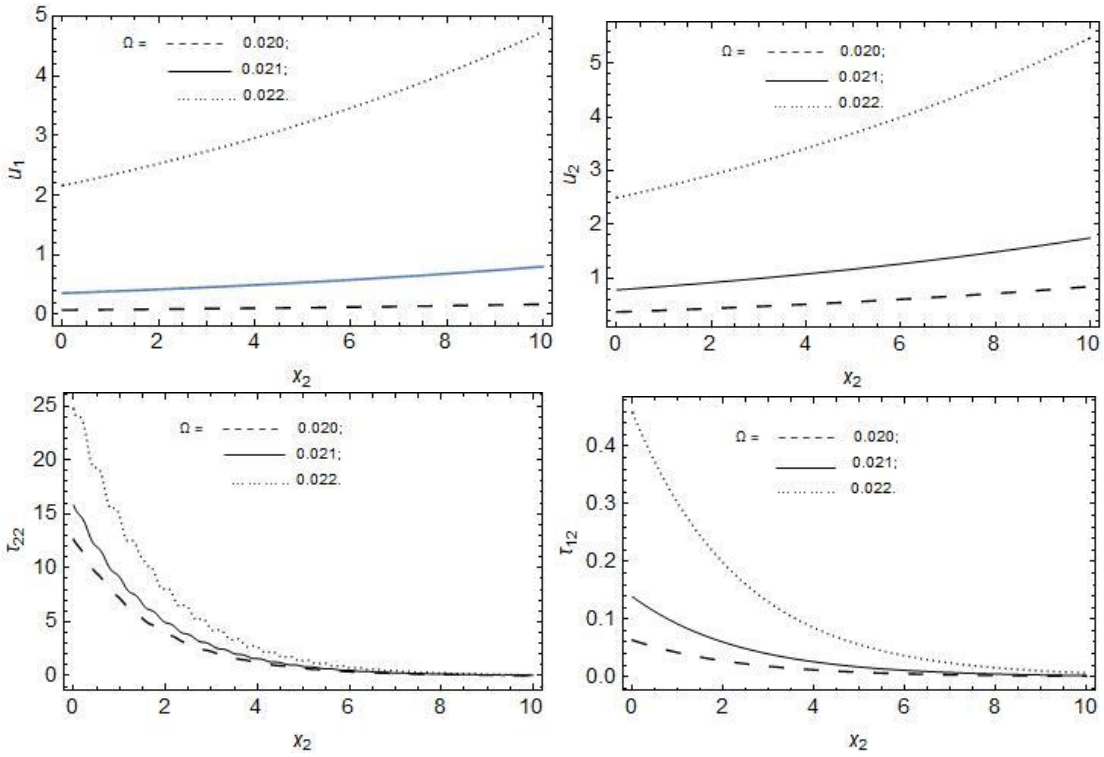
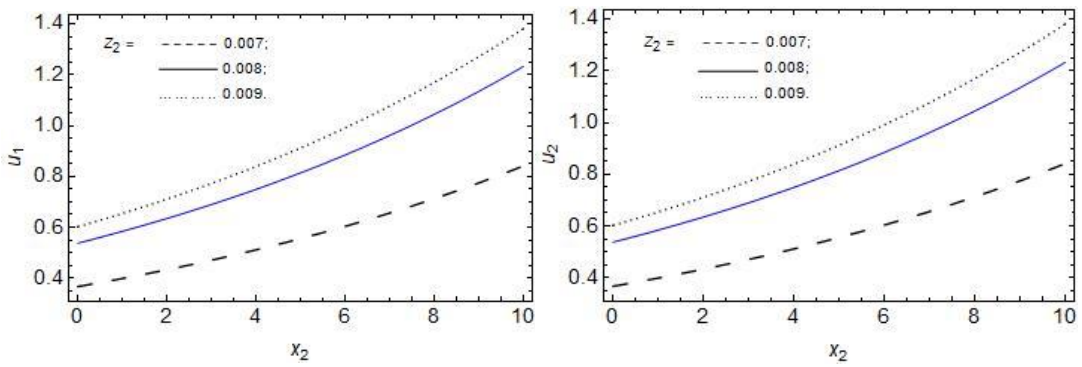


Fig. 7: Impact of distinct rotation $\Omega rad/s$ on the displacement components $u_i, i=1,2$, normal stress τ_{22} and shear stress τ_{12} versus x_2 in meters.

surface Fig. 7 shows the effects of rotation Ω on the displacements $u_i, i=1,2$, normal stress τ_{22} and shear stress τ_{12} versus x_2 coordinate in meters following a steady interaction of the physical quantities or physical parameters of inclined angle θ, mechanical inclined parameter F_0 (applied force), magnetic field $H_0(A/m)$, inhomogeneous parameter m, inhomogeneous impedance $Z_i, \mathrm{i}=1,2$ and corrugated parameters a,b at a given time t on the material. We deduce that in Fig. 7, an increase in behaviors of the displacements $u_i, i=1,2$, and stresses τ_{22} and τ_{12} on the material are witnessed for increase in rotation Ω of the medium. The maxima values of the stresses on the material are attained when the rotation Ω of the medium increase near the origin whereas the maxima values for the displacements are achieved close to vanishing domain of the wave propagation on the material, that is, close to $x_2=10$ when the rotation is $\Omega=0.022$.



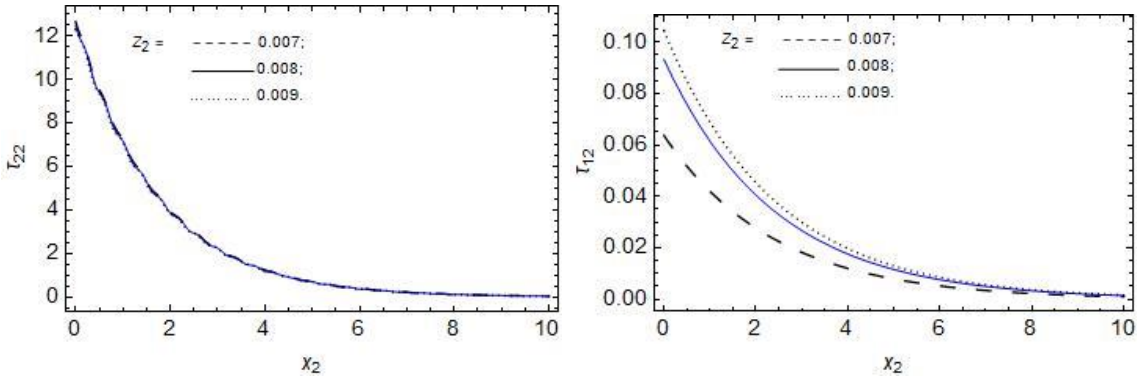
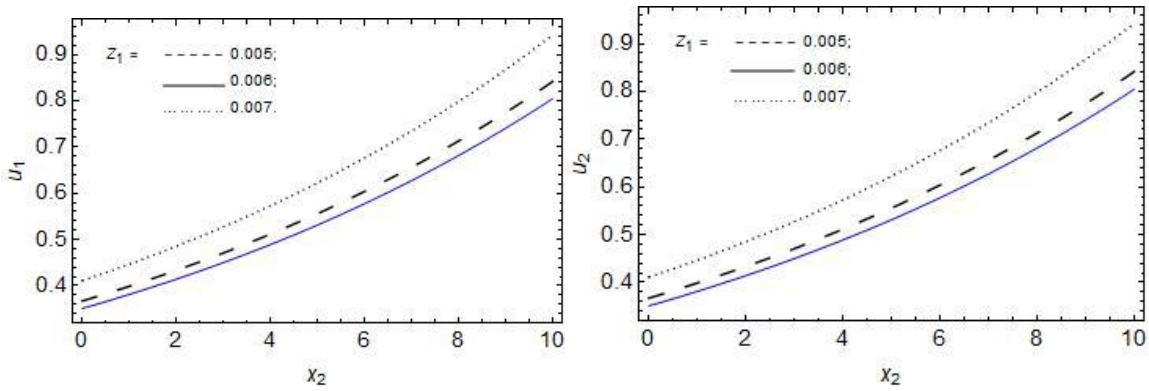


Fig. 8: Impact of distinct inhomogeneous impedance Z_2 on the displacement components $u_i, i = 1,2$, normal stress τ_{22} and shear stress τ_{12} versus x_2 in meters.

In spite of this, Fig. 8 depicts the impact of inhomogeneous impedance Z_2 on the displacements $u_i, i = 1,2$, normal stress τ_{22} and shear stress τ_{12} versus x_2 coordinate based on a constant application of the interacting physical quantities of rotation Ω, inclined angle θ, mechanical inclined parameter F_0 (applied force), magnetic field H_0, inhomogeneous parameter m, horizontal inhomogeneous impedance Z_1, and corrugated parameters a, b on the fibre-reinforced material at a given time t. We observe that increase in the normal or vertical impedance Z_2 led to increase in behavior of the displacements $u_i, i = 1,2$ and shear stress τ_{12} on the material while noting a negligible effect on the normal component of stress at this instance. Physically speaking, we can adduce the effect of the impedance along the normal of the material which has weighed in to cause a resistant-like effect on the normal stress of the propagating wave. We found also, that the maxima values of the displacements lies near $x_2 = 10$, that is, end part of the material where the propagating wave vanishes while the maxima for the stresses were found to lie near the origin especially for increased normal impedance Z_2 on the fibre-reinforced body.



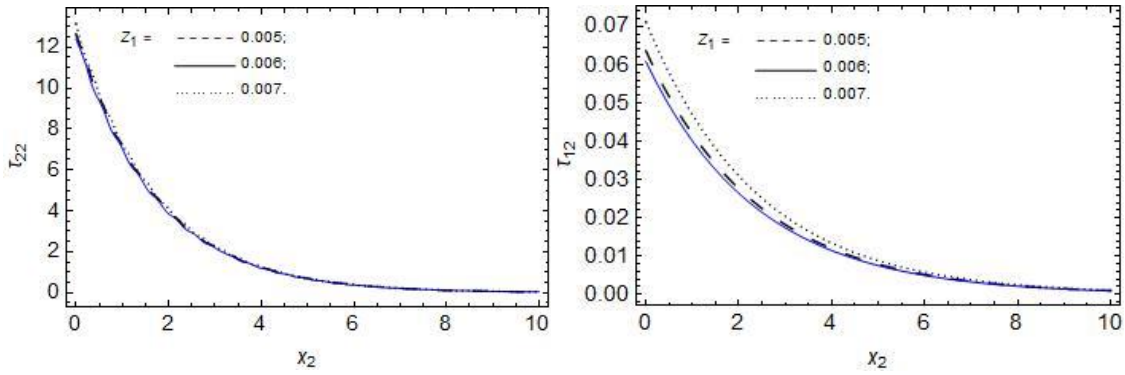


Fig. 9: Impact of distinct inhomogeneous impedance Z_1 on the displacement components $u_i, i = 1,2$, normal stress τ_{22} and shear stress τ_{12} versus x_2 in meters.

Also, Fig. 9 demonstrate the impact of inhomogeneous impedance Z_1 on the displacements $u_i, i = 1,2$, normal stress τ_{22} and shear stress τ_{12} versus x_2 coordinate through a constant application of the interacting physical quantities of rotation Ω, inclined angle θ, mechanical inclined parameter F_0 (applied force), magnetic field H_0, inhomogeneous parameter m, normal inhomogeneous impedance Z_2, and corrugated parameters a, b on the fibre-reinforced material at a given time t. We observe that increase in the horizontal impedance Z_1 increase the behavior of the displacements $u_i, i = 1,2$ and stresses on the material especially when $Z_1 = 0.007$. For $x_2 > 3$ we equally note a near negligible effect on the normal component of stress at this instance. Generally, all the fields' distributions have gradual mixed behaviors (increase and decrease) for an increase in Z_1. We found also, that the maxima values of the displacements lies near $x_2 = 10$, that is, end length of the material where the propagating wave vanishes while the maxima for the stresses were found to lie near the origin especially for increased impedance Z_1 on the fibre-reinforced medium.

Conclusion

A mathematical approach that seek to analyze surface waves in a rotating inhomogeneous impedance-corrugated surface under inclined mechanical load and magnetism is the hallmark of this investigation. In studying this, we developed the dynamical equations through constitutive laws of stress-strain relations involving inhomogeneous fibre-reinforced medium. The inhomogeneity is occasioned by the exponentially decaying material parameters. Subsequently, we derived using the normal mode approach, the analytical solutions of the fields' distributions of displacements and stresses of the surface wave propagating on the material whilst observing non-dimensionalization of the dynamical equations or equations of motion. Computational results which showed impacts of the considered physical parameters; inhomogeneous parameter m, rotation Ω of the material, magnetic field H_0, angle of inclinations θ, etc. on the inhomogeneous impedance-corrugated surface material in graphical forms are presented. This stems from the fact that the observations made for the combined contributing physical parameters depicts great impacts on the stresses and displacements of the surface wave on the inhomogeneous fibre-reinforced material. Thus, it follows that:

i. Increase in rotation Ω, mechanical inclined parameter F_0 (applied force) and mechanical angle of inclination θ produce corresponding increase in the behavior of the displacements and stresses of the wave on the material.

ii. The amplitude a of the corrugated surface increase the shear stress τ_{12}, and the displacements of the wave on the medium especially when increased while the normal stress τ_{22} demonstrate mixed behavior. Also, the wave number b of the corrugation caused mixed behaviors on the normal stress and displacement profiles $u_i, i = 1,2$, of the wave when increased. More so, τ_{22} demonstrate decrease behavior in an oscillating manner when the wave number is high, that is, for $b = 0.7$ in the domain $x_2 \leq 0.4$.

iii. The magnetic field H_0 impacts the shear stress τ_{12} and displacements of the wave on the material in mixed behavior (increase and decrease) when varied in an increase manner. Also, it influences in a decreasing behavior on the normal stress τ_{22} when increased.

iv. Increase in the inhomogeneity m on the material decrease the normal stress τ_{22} on the material while noting mixed behavior in the domain $0 < x_2 \leq 1$ where the maximum value lies. In addition, inhomogeneity m of the material caused clear mixed behavior (increase and decrease) on the displacements $u_i, i = 1,2$ and the shear stress τ_{12} when increased on the material.

v. Increase in the inhomogeneous impedance Z_1, yielded maximum and gradual increase in behavior on the displacements and stresses of the waves on the fibre-reinforced medium. However, a resistant-like effects were observed along the normal stress components when the inhomogeneous normal impedance Z_2 is increased.

Sequel to this, interesting known cases of this study could be visualized if the inhomogeneous parameter is neglected both on the material body and on the impedance conditions at the corrugated boundary surface. This would lead to fibre-reinforced solutions with the interacting physical quantities in homogeneous form. In fact, it is eminent to posit that this study would be of essence to the scientists in virtually all physical sciences, engineering, among others, where mathematical wave solutions and analysis associated with stress and displacement distributions on inhomogeneous and homogeneous fibre-reinforced materials with imperfect surfaces are paramount and examined.

References

[1] Abd-Alla, A. M., Abo-Dahab. S. M. and khan. A. (2017). Rotational effects on magneto-thermoelastic stonely, Love, and Rayleigh waves in fibre-reinforced anisotropic general viscoelastic media of higher order CMC, 53, pp.49–72.

[2] Abd-Alla, A. M., Abo-Dahab. S. M., Alotaibi. Hind. A. (2016): Effect of the Rotation on a Non-Homogeneous Infinite Elastic Cylinder of Orthotropic Material with Magnetic Field, J. Comput. Theor. Nanosci, 3, 4476-4492. doi:10.1166/jctn.2016.5308

[3] Ailawalia. P., Sachdeva S. K. and Pathania. D. (2015). A two dimensional fibre reinforced micropolar thermoelastic problem for a half-space subjected to mechanical force Theor. Appl. Mech, 42, 11-25. DOI:10.2298/TAM1501011A

[4] Anya, A.I., Akhtar, M.W., Abo-Dahab,M.S., Kaneez, H., Khan, A. and Adnan, J. (2018). Effects of a magnetic field and initial stress on reflection of SV-waves at a free surface with voids under gravity. J. Mech. Behav. Mater., 27, 5–6. . https://doi.org/10.1515/jmbm-2018-0002

[5] Anya, A.I., and Khan, A. (2019). Reflection and propagation of plane waves at free surfaces of a rotating micropolar fibre-reinforced medium with voids, Geomech. & Eng. 18, 605–614.

[6] Anya, A. I., and Khan, A. (2020). Reflection and propagation of magneto-thermoelastic plane waves at free surfaces of a rotating micropolar fibre-reinforced medium under G-L theory.- Int. J. of Acoust. and Vib., 25, 190-199. https://doi.org/10.20855/ijav.2020.25.21575

[7] Anya, A. I., and Khan, A. (2022). Plane waves in a micropolar fibre-reinforced solid and liquid interface for non-insulated boundary under magneto-thermo-elasticit, J. Comput. Appl. Mech., 53, pp.204-218. doi:10.22059/jcamech.2022.341656.712

[8] Anya, A. I., Nwachioma, C., and Ali, H. (2023). Magnetic effects on surface waves in a rotating non-homogeneous hal-space with grooved and impedance boundary characteristics, Int. Appl. J. Appl. Mech., 28(4), 26-42.

[9] Asano, S. (1966). Reflection and refraction of elastic waves at a corrugated interface.-Bull. Seism.Soc. Am., 56, pp.201-221.

[10] Azhar, E., Ali, H., Jahangir, A., and Anya, A. I., (2023). Effect of Hall current on reflection of magneto-thermoelastic waves in a non-local semiconducting solid, Waves in random and complex media, 1-18, https://doi..org/10.1080/17455030.2023.2182146.

[11] Chattopadhyay, A. (1975). On the dispersion equation for Love wave due to irregularity in the thickness of non-homogeneous crustal layer.- Acta Geol. Pol., 23, 307-317.

[12] Chowdhury S., Kundu S., Alam P. and Gupta, Sh.(2021): Dispersion of Stoneley waves through the irregular common interface of two hydrostatic stressed MTI medi.- Scientia Iranica, 28, 837-846. doi:10.24200/SCI.2020.52653.2820.

[13] Das, S.C., Acharya, D. P., and Sengupta, D. R. (1992). Surface waves in an inhomogeneous elastic medium under the influence of gravity, Rev Roumaine Sci. Tech. Ser. Mec. Appl., 37, 539-551.

[14] Giovannini, L.(2022): Theory of dipole-exchange spin-wave propagation in periodically corrugated films.- Phys. Rev. B, 105, 214426 doi.org/10.1103/PhysRevB.105.214426.

[15] Gupta, R. R. (2014). Surface wave characteristics in a micropolar transversely isotropic half-space underlying an inviscid liquid layer.- Int. J. of Appl. Mech. Eng., vol.19, pp.49–60.

[16] Gupta, R. R. (2014). Surface wave characteristics in a micropolar transversely isotropic half-space underlying an inviscid liquid layer.-Int. J. of Appl. Mech. Eng., vol.19, pp.49–60.

[17] Khan, A., Anya, A. I., and Kaneez, H. (2015). Gravitational effects on surface waves in non-homogeneous rotating fibre-reinforced anisotropic elastic media with voids.- Int. J. Appl. Sci. Eng. Res.,4, 620–632.

[18] Maleki, F., and Jafarzadeh, F. (2023). Model tests on determining the effect of various geometrical aspects on horizontal impedance function of surface footings, Scientia Iranica, In Press, doi:10.24200/SCI.2023.59744.6403.

[19] Munish S., Sharma A., Sharma A. (2016): Propagation of SH Waves in a Double Non-Homogeneous Crustal Layers of Finite Depth Lying Over an homogeneous Half-Space, Lat. Am. J. Solids Struct.,13, 2628-2642. https://doi.org/10.1590/1679-78253005

[20] Rakshit, S., Mistri, K. C., Das, A. and Lakshman A. (2022). Effect of interfacial imperfections on SH-wave propagation in a porous piezoelectric composit.- Mech. Adv. Mater. Struct., 29, 4008-4018. doi.org/10.1080/15376494.2021.1916138.

[21] Rakshit, S., Mistri, K.C., Das, A. and Lakshman, A. (2021). Stress analysis on the irregular surface of visco-porous piezoelectric half-space subjected to a moving load.- J. Intell. Mater. Syst. Struct., 33, 1244-1270. https://doi.org/10.1177/1045389X211048226.

[22] Roy, I., Acharya D.P. and Acharya, S. (2017). Propagation and reflection of plane waves in a rotating magneto-elastic fibre-reinforced semi space with surface stress. Mech. & Mech. Eng., 21, pp.1043–1061 (2017). DOI:10.2478/mme-2018-0074

[23] Schoenberg, M. and Censor, D. (1973). Elastic waves in rotating media. Quart. Appl. Math. 31 , 115–125.

[24] Singh, B. (2016). Reflection of elastic waves from plane surface of a half-space with impedance boundary conditions, Geosci. Res., 2, 242-253.

[25] Singh, S. S., and Tomar S. K. (2008). qP-wave at a corrugated interface between two dissimilar pre-stressed elastic half-spaces.- J. Sound Vib., 317(3): 687-708.

[26] Singh, A. K., Das, A., Kumar, S. and Chattopadhyay, A. (2015). Influence of corrugated boundary surfaces reinforcement, hydrostatic stress, heterogeneity and anisotropy on Love type wave propagation.-Meccanica vol.50, pp.2977-2994. . doi:10.1007/s11012-015-0172-6

[27] Singh, A. K., Mistri K. C., and Mukesh, P. K. (2018). Effect of loose bonding and corrugated boundary surface on propagation of rayleigh-type wave. Lat. Am. J. Solids Struct., vol.15, e01.

[28] Singh, D. and Sindhu R. (2011). Propagation of waves at interface between a liquid half- space and an orthotropic micropolar solid half-space. Adv. Acoust. And Vib. 2011, 1–5.

[29] Singh, B., and Kaur, B. (2022). Rayleigh surface wave at an impedance boundary of an incompressible micropolar solid half-spac.- Mech. Adv. Mater. Struct., 29, pp. 3942-3949.

[30] Singh, B. and Kaur, B. (2020). Rayleigh-type surface wave on a rotating orthotropic elastic half-space with impedance boundary conditions.- J. Vib. Control., vol. 26, pp. 1980- 1987.

[31] Sahu S.A., Mondal S. and Nirwal S. (2022). Mathematical analysis of Rayleigh waves at the nonplanner boundary between orthotropic and micropolar media.- Int. J. Geomech., 23, doi.org/10.1061/IJGNAI.GMENG-7246.

[32] Spencer, A. J. M. (1972). Deformations of fibre-reinforced materials, Oxford Uni. Pres. Lond.

[33] Sunita, D., Suresh, K. S., and Kapil K. K. (2019). Reflection at the free surface of fibre-reinforced thermoelastic rotating medium with two temperature and phase-lag.- Appl. Math. Model., 65,106–119. https://doi.org/10.1016/j.apm.2018.08.004

[34] Barak, M. S. and Dhankhar, P., (2023). Thermo-mechanical interactions in a rotating nonlocal functionally graded transversely isotropic elastic half-space, ZAMM-Journal of Applied Mathematics and Mechanic/Zeitschrift für Angewandte Mathematik und Mechanik, Vol.103(2). https://doi.org/10.1002/zamm.202200319

[35] Barak, M. S, Poonia, R., Devi, S. Dhankhar, P. (2024). Nonlocal and dual-phase-lag effects in a transversely isotropic exponentially graded thermoelastic medium with voids, ZAMM-Journal of Applied Mathematics and Mechanics / Zeitschrift für Angewandte Mathematik und Mechanik, 104, 5, https://doi.org/10.1002/zamm.202300579

[36] Anya, A. I. and Khan, A. (2019). Propagation and reflection of magneto-elastic plane waves at the free surface of a rotating micropolar fibre-reinforced medium with voids, Journal of Theoretical and Applied Mechanics, vol. 57. https://doi.org/10.15632/jtam-pl/112066

Appendix

$$C_{11} = A_{13}A_{15};$$

$$C_{12} = -m\left(A_{15}A_{24} + A_{13}A_{27}\right);$$

$$C_{13} = (-b^2 i^2 \rho A_{12}^2 - b^2 \rho A_{15} - \rho\omega^2 A_{15} + \rho^2\Omega^2 A_{15} + m^2 \rho A_{24}A_{27} - \omega^2 A_{15}H_0^2\varepsilon_0\mu_0^2 + A_{13}(-\rho\omega^2 + \rho^2\Omega^2 - b^2\rho A_{13} - \omega^2 H_0^2\mu_0^2))/\rho;$$

$$C_{14} = (m(b^2 i^2 \rho A_{12}A_{26} + A_{24}(\rho\omega^2 - \rho^2\Omega^2 + b^2 i^2 \rho A_{12} + b^2\rho A_{13} + \omega^2 H_0^2\mu_0^2) + A_{27}\left(\rho\left(b^2 + \omega^2 - \rho\Omega^2\right) + \omega^2 H_0^2\varepsilon_0\mu_0^2\right)))/\rho$$

$$C_{15} = \frac{1}{\rho^2}(b^2\rho^2\omega^2 + \rho^2\omega^4 - b^2\rho^3\Omega^2 - 2\rho^3\omega^2\Omega^2 + 4\rho^4\omega^2\Omega^2 + \rho^4\Omega^4 - 2bim\rho^3\omega\Omega A_{26} + bim\rho^2 A_{24}\left(2\rho\omega\Omega - bimA_{26}\right) + b^2\rho\omega^2 H_0^2\mu_0^2 + \rho\omega^4 H_0^2\mu_0^2 - \rho^2\omega^2\Omega^2 H_0^2\mu_0^2 + \rho\omega^4 H_0^2\varepsilon_0\mu_0^2 - \rho^2\omega^2\Omega^2 H_0^2\varepsilon_0\mu_0^2 + \omega^4 H_0^4\varepsilon_0\mu_0^4 + b^2\rho A_{13}\left(\rho\left(b^2 + \omega^2 - \rho\Omega^2\right) + \omega^2 H_0^2\varepsilon_0\mu_0^2\right));$$